Am J Physiol Lung Cell Mol Physiol 303: L343–L353, 2012.
First published June 8, 2012; doi:10.1152/ajplung.00130.2012.

Hypoxia-induced migration in pulmonary arterial smooth muscle cells requires calcium-dependent upregulation of aquaporin 1

Kyle Leggett,[1] Julie Maylor,[1] Clark Undem,[1] Ning Lai,[1,3] Wenju Lu,[1] Kelly Schweitzer,[1] Landon S. King,[1] Allen C. Myers,[2] J. T. Sylvester,[1] Venkataramana Sidhaye,[1] and Larissa A. Shimoda[1]

[1]*Division of Pulmonary and Critical Care Medicine, Department of Medicine, Johns Hopkins School of Medicine, Baltimore, Maryland;* [2]*Division of Allergy and Immunology, Department of Medicine, Johns Hopkins School of Medicine, Baltimore, Maryland; and* [3]*Guangzhou Institute of Respiratory Diseases, State Key Laboratory of Respiratory Diseases, The First Affiliated Hospital, Guangzhou Medical University, Guangzhou, People's Republic of China*

Submitted 23 April 2012; accepted in final form 6 June 2012

Leggett K, Maylor J, Undem C, Lai N, Lu W, Schweitzer K, King LS, Myers AC, Sylvester JT, Sidhaye V, Shimoda LA. Hypoxia-induced migration in pulmonary arterial smooth muscle cells requires calcium-dependent upregulation of aquaporin 1. *Am J Physiol Lung Cell Mol Physiol* 303: L343–L353, 2012. First published June 8, 2012; doi:10.1152/ajplung.00130.2012.—Pulmonary arterial smooth muscle cell (PASMC) migration is a key component of the vascular remodeling that occurs during the development of hypoxic pulmonary hypertension, although the mechanisms governing this phenomenon remain poorly understood. Aquaporin-1 (AQP1), an integral membrane water channel protein, has recently been shown to aid in migration of endothelial cells. Since AQP1 is expressed in certain types of vascular smooth muscle, we hypothesized that AQP1 would be expressed in PASMCs and would be required for migration in response to hypoxia. Using PCR and immunoblot techniques, we determined the expression of AQPs in pulmonary vascular smooth muscle and the effect of hypoxia on AQP levels, and we examined the role of AQP1 in hypoxia-induced migration in rat PASMCs using Transwell filter assays. Moreover, since the cytoplasmic tail of AQP1 contains a putative calcium binding site and an increase in intracellular calcium concentration ($[Ca^{2+}]_i$) is a hallmark of hypoxic exposure in PASMCs, we also determined whether the responses were Ca^{2+} dependent. Results were compared with those obtained in aortic smooth muscle cells (AoSMCs). We found that although AQP1 was abundant in both PASMCs and AoSMCs, hypoxia selectively increased AQP1 protein levels, $[Ca^{2+}]_i$, and migration in PASMCs. Blockade of Ca^{2+} entry through voltage-dependent Ca^{2+} or nonselective cation channels prevented the hypoxia-induced increase in PASMC $[Ca^{2+}]_i$, AQP1 levels, and migration. Silencing AQP1 via siRNA also prevented hypoxia-induced migration of PASMCs. Our results suggest that hypoxia induces a PASMC-specific increase in $[Ca^{2+}]_i$ that results in increased AQP1 protein levels and cell migration.

AQP1; vascular smooth muscle

THE PROLONGED HYPOXIC EXPOSURE associated with many chronic lung diseases has adverse effects on the pulmonary vasculature and, consequently, results in the development of pulmonary hypertension. Under conditions of chronic hypoxia (CH), the increased pulmonary vascular resistance and subsequent elevation in pulmonary arterial pressure are due to sustained smooth muscle contraction and vascular remodeling (23). Remodeling and restructuring of the pulmonary blood vessels have been shown to be characterized by thickening of the medial layer of muscular vessels and extension of muscle into previously nonmuscular small precapillary arterioles, likely resulting from proliferation and migration of pulmonary arterial smooth muscle cells (PASMCs) and cellular transdifferentiation (i.e., endothelial-mesenchymal transformation) (24, 29). Despite extensive study, the mechanisms underlying these functional consequences of CH remain poorly understood.

Aquaporins (AQPs) are a family of integral membrane proteins that form pores and regulate the movement of water, and in select cases some small solutes, into and out of the cell in response to osmotic gradients. The structure of all 13 AQP family members (AQP0–12) consists of six transmembrane α-helices arranged such that both the COOH-terminal and NH_2-terminal domains are located in the cytoplasm (9). Recently, aquaporin-1 (AQP1) was found to be required for migration of endothelial, epithelial, and tumor cells (7, 8, 13, 15, 18), although the mechanism of action remains poorly understood. Although AQP1 has been shown to be expressed in aortic and coronary vascular smooth muscle (20), the distribution of AQPs in PASMCs, and their function in these cells, has yet to be determined.

A hallmark of hypoxic exposure in PASMCs is an increase in intracellular $[Ca^{2+}]_i$ concentration ($[Ca^{2+}]_i$) (reviewed in Refs. 21, 25). In contrast, systemic smooth muscle cells respond to hypoxia with no change or a decrease in $[Ca^{2+}]_i$ (5, 19, 28, 31, 35). The COOH-terminal tail of AQP1 contains a putative E-F hand motif that would allow binding of cytosolic Ca^{2+} and, therefore, possible regulation of AQP1 by $[Ca^{2+}]_i$ (6). Thus, in the present study, we hypothesized that AQP1 is present in the pulmonary vasculature and that the hypoxia-induced increase in $[Ca^{2+}]_i$ would induce AQP1-dependent migration in PASMCs. To test this hypothesis, we first used RT-PCR and immunoblot analysis to measure AQP expression in pulmonary arteries and PASMCs, compared this expression pattern to aortic smooth muscle cells (AoSMCs), and determined the effect of hypoxia on AQP levels. We then used Transwell assays to measure cell migration and fluorescent microscopy to measure $[Ca^{2+}]_i$ under both normoxic and hypoxic conditions in AoSMCs and PASMCs. Finally, we evaluated the effect of Ca^{2+} channel blockers on AQP1 expression and migration, as well as the effect of AQP1 depletion with small interfering RNA (siRNA) on hypoxia-induced migration in PASMCs.

METHODS

In vivo exposure to CH. All protocols were reviewed and approved by the Johns Hopkins University Animal Care and Use Committee.

Address for reprint requests and other correspondence: L. A. Shimoda, Division of Pulmonary and Critical Care Medicine, Johns Hopkins Univ., 5501 Hopkins Bayview Circle, JHAAC 4A.52, Baltimore, MD 21224 (e-mail: shimodal@welch.jhu.edu).

Adult, male Wistar rats (250–300 g) were placed in a chamber maintained at 10% O_2 for 3 wk, as previously described (32). The chamber was constantly flushed with room air to maintain low (<0.5%) CO_2 concentrations. A servo-control system (PRO-OX, RCI Hudson) monitored O_2 levels and injected 100% N_2 as needed to maintain 10 ± 0.5% O_2. Cages were cleaned and food and water replenished twice a week. Normoxic animals were kept in room air on a wire rack adjacent to the chamber. Animals were exposed to a natural light-dark cycle and allowed free access to food and water.

Isolation and culture of smooth muscle cells. Rats were anesthetized with pentobarbital sodium (130 mg/kg ip). The lungs were removed and dissected in HBSS containing 130 mM KCl, 5 mM $MgCl_2$, 10 mM HEPES, 1.5 mM $CaCl_2$, and 10 mM glucose with pH adjusted to 7.2 with 5 M NaOH. Intrapulmonary arteries (200–600 μm outer diameter) and a segment of the thoracic aorta were removed and cleaned of adventia, and the lumen was gently swiped with a cotton-tipped swab to remove endothelial cells. The arteries were then placed in 4°C HBSS for 30 min to recover and subsequently placed in reduced-calcium HBSS (20 μm $CaCl_2$) at room temperature. Next, the tissue was digested in reduced-calcium HBSS containing type I collagenase (1,750 U/ml), papain (9.5 U/ml), bovine serum albumin (2 mg/ml), and DTT (1 mM) at 37°C for 20 min in the case of PASMCs or 40 min in the case of aortic smooth muscle cells (AoSMCs). Lastly, the tissue was triturated in Ca^{2+}-free HBSS and cells were placed in culture dishes with SMBM medium (Lonza) supplemented with 0.3% FCS and 1% penicillin-streptomycin for 48 h. In some experiments, cells were then placed into SmGM Complete medium (Lonza) and grown to 80% confluence (24–96 h) before being placed in low-serum (0.3% FCS) medium for 48 h and then being exposed to either hypoxic or normoxic conditions in a modular incubator. In vitro exposure to hypoxia was achieved by placing cells in an airtight chamber (Billups-Rothberg) gassed with 4% O_2-5% CO_2. The chamber and the normoxic control plates were placed in an incubator at 37°C. Initial experiments were performed by using a hand-held oxygen monitor (model 5577; Hudson RCI) to verify that the chamber was able to sustain the desired level of hypoxia for a minimum of 48 h.

Conventional and real-time RT-PCR. Total RNA was extracted from cells by use of the RNeasy Mini kit (Qiagen) and stored at −80° C. Reverse transcription was performed using the First-Strand cDNA kit (Bio-Rad) containing reverse transcriptase, dNTPs, nuclease free-water, and buffer. For conventional PCR, reactions were made by using 5 μl $MgCl_2$ buffer, 1.5 μl $MgCl_2$, 1 μl dNTPs, 3 μl cDNA, and 2 μl reverse and forward primers and added to the PCR Thermocycler for 40 cycles. Primer sequences specific for the genes of interest were designed using Primer3 software (http://frodo.wi.mit.edu/) and are listed in Table 1. Each product was run on a 1% ethidium bromide agarose gel and imaged with ultraviolet light. After imaging, the bands were excised and sent for sequencing at the Johns Hopkins Sequencing facility to confirm product specificity. For quantification, real-time RT-PCR was performed using the QuantiTect SYBR Green Kit (Qiagen). Specificity of real-time PCR products was confirmed by observation of a single peak in the melting curve performed after cDNA amplification and a single band of expected size on an agarose gel, which was then excised and sequenced. Relative concentrations of each gene were calculated using the Pfaffl method (16), where PCR detection threshold cycle (C_T) values for each plate were calculated by using iCycler (Bio-Rad) software and efficiencies for each primer pair were calculated from a fivefold serial dilution standard curved performed for each gene during each RT-PCR run. Data are expressed as a ratio of gene of interest to housekeeping gene (cyclophilin B; CpB) within a sample and normalized to the value of the control sample.

Immunoblot analysis. For tissue, lungs were perfused free of blood and homogenized as previously described (10). Cells were washed with PBS; protein was extracted in Laemmli sample lysis buffer containing 200 μM 4-(2-aminoethyl) benzenesulfonyl fluoride hydrochloride, 1 mM EDTA, and protease inhibiter cocktail; and the protein was stored at −80°C. Proteins (10–25 μg) were separated on 12% SDS acrylamide gels, transferred to polyvinylidene fluoride membranes, and blocked in 5% nonfat dry milk. Membranes were the probed with primary and secondary antibodies and bands visualized by ECL (Amersham) according to the manufacturer's instructions. Densitometry was used to quantify protein levels. The primary anti-

Table 1. *PCR primers*

Gene	Accession Number	Source	Primer Pair Sequence (Sense/Antisense)	Product Size, bp
			Conventional	
AQP1	NM_012778	Rat	5′-GGCTTGTCTGTGGCTCTTG-3′ 5′-ATCATCAGCATCCAGGTCATAC-3′	261
AQP2	NM_012909	Rat	5′-AGTGCTGGCTGAGTTCTTG-3′ 5′-TGGCGTTGTTGTGGAGAG-3′	341
AQP3	NM_031703	Rat	5′-GTGGTTCCGTGGCTCAAG-3′ 5′-CCATATCCAAGTGTCCAGAGG-3′	354
AQP4	NM_012825	Rat	5′-ATCGCCAAGTCTGTCTTCTAC-3′ 5′-ACGGAACCAGTAACATCAGTC-3′	233
AQP6	NM_022181	Rat	5′-ATCTACTTCACTGGCTGTTCC-3′ 5′-GTGTCCTCTGAGTTCGTCTG-3′	263
AQP7	NM_019157	Rat	5′-GCTATCTTGGTGTCAACTTGG-3′ 5′-GTGCTGGACTGTTCAACTTG-3′	396
AQP8	NM_019158	Rat	5′-AGACGCCGATGTGTAGTATG-3′ 5′-GCCTCCAACCAGTGTGAC-3′	305
AQP9	NM_022960	Rat	5′-GCAGTCGTGATGGCTCTC-3′ 5′-ACCTGGCGTGGATATGAATG-3′	282
			Real-time	
AQP1	NM_012778	Rat	5′-GGACGAGTGACCTTTGGACT-3′ 5′-TGACACGATGGAACTTGCTG-3′	118
AQP4	NM_012825	Rat	5′-CGGTTCATGGAAACCTCACT-3′ 5′-CATGCTGGCTCCGGTATAAT-3′	191
AQP7	NM_019157	Rat	5′-GCAGGTGGAGAACTGTTGGT-3′ 5′-GGAGCATCCCAGTCACAAAT-3′	127
CpB	NM_022536	Rat	5′-CCGAGACTTAGGTGGCTCAG-3′ 5′-TTGATCCCACAGCCAGTGTA-3′	93

bodies used were AQP1 (Alpha Diagnostics), AQP4 (Abcam), AQP7 (LSBio), smooth muscle-specific α-actin (Sigma), Na^+-K^+-ATPase (Millipore), and AQP5 (14).

Migration assays. Cell migration was assessed in two assays: scratch (wound) motility assay (qualitative) and Transwell filter (quantitative). For the scratch motility assay, cells were grown to confluence on glass coverslips and placed into basal medium for 48 h. Cells were then removed from the middle section of the confluent monolayer by a single pass with a 1,000-μl pipette tip, washed with PBS, placed in fresh basal medium (0.3% FBS), and incubated with 5 μM calcein (Invitrogen) for 1 h. Extracellular calcein was removed by placing cells into fresh basal medium and images were taken on an inverted microscope at a magnification of ×40 (*time 0*). Cells were then incubated under control (20% O_2) or hypoxic (4% O_2) conditions and cells reimaged after 24 h. For Transwell assays, 50,000–100,000 cells were added to the top of a polycarbonate filter with 8-μm pores in 4 ml of basal medium. The cells were incubated for 24 h under control or hypoxic conditions. Following exposure, the cells were fixed in 95% ethanol for 10 min and stained with brilliant blue (Pierce) for 5 min. Cells were visualized via microscope mounted camera and Q-capture software. For each filter, five randomly chosen fields were imaged to obtain a total cell count. Unmigrated cells were then scraped off the top of the filter and the migrated cells (bottom layer) were imaged. Migration was calculated as the percent of cells remaining normalized to total number of cells on the filter.

Measurement of $[Ca^{2+}]_i$. Cells were incubated with 7.5 μM fura 2-AM for 60 min at 37°C, placed in a closed, heated chamber on the stage of an inverted microscope (Nikon TSE 100 Eclipse) and superfused with modified Krebs solution containing (in mM) 118 NaCl, 4.7 KCl, 0.57 $MgSO_4$, 1.18 KH_2PO_4, 25 $NaHCO_3$, 2.5 $CaCl_2$, and 10 glucose and bubbled with 16% O_2-5% CO_2 at 38°C. PASMCs were perfused for 15 min prior to beginning experiments to remove extracellular dye. Fura 2 fluorescence was measured in cells excited at 340 and 380 nm via a ×20 fluorescence objective and an electronic shutter to minimize photobleaching. Emitted light was detected at 510 nm by an imaging camera. Protocols were executed and data collected online with InCyte software (Intracellular Imaging). $[Ca^{2+}]_i$ was calculated from fura 2 fluorescence ratios by using a five-point calibration curve generated with commercial calibration solutions (Molecular Probes).

siRNA transfection. siRNA targeting AQP1 and nontargeting siRNA (control) were obtained as a "smart pool" from Dharmacon. Cells were incubated with 100 nM of siRNA for 6 h in serum- and antibiotic-free medium. Serum was then added to the medium to bring the total concentration to 10% FCS and cells incubated for 24 h. The medium was then changed to low serum (0.3% FCS) for an additional 48 h, after which cells were harvested for protein analysis or migration assays.

Lung histology/immunofluorescence. A suture was used to occlude the right lung, which was removed for isolation of PASMCs. A cannula was inserted into the trachea and the left lung was inflated with 0.75 ml of 10% formalin, placed in formalin overnight, transferred to 70% ethanol, embedded in paraffin, and sectioned into 5-μm slices. Sections were subjected to antigen retrieval, blocked, stained with anti-smooth muscle-specific α-actin primary antibody (SMA; Sigma-Aldrich) overnight at 4°C, and incubated with Cy3-conjugated secondary antibody (Molecular Probes) for 1 h at room temperature. Each lung section was evaluated by an investigator blinded to condition for the presence of SMA-positive small-diameter vessels (outer

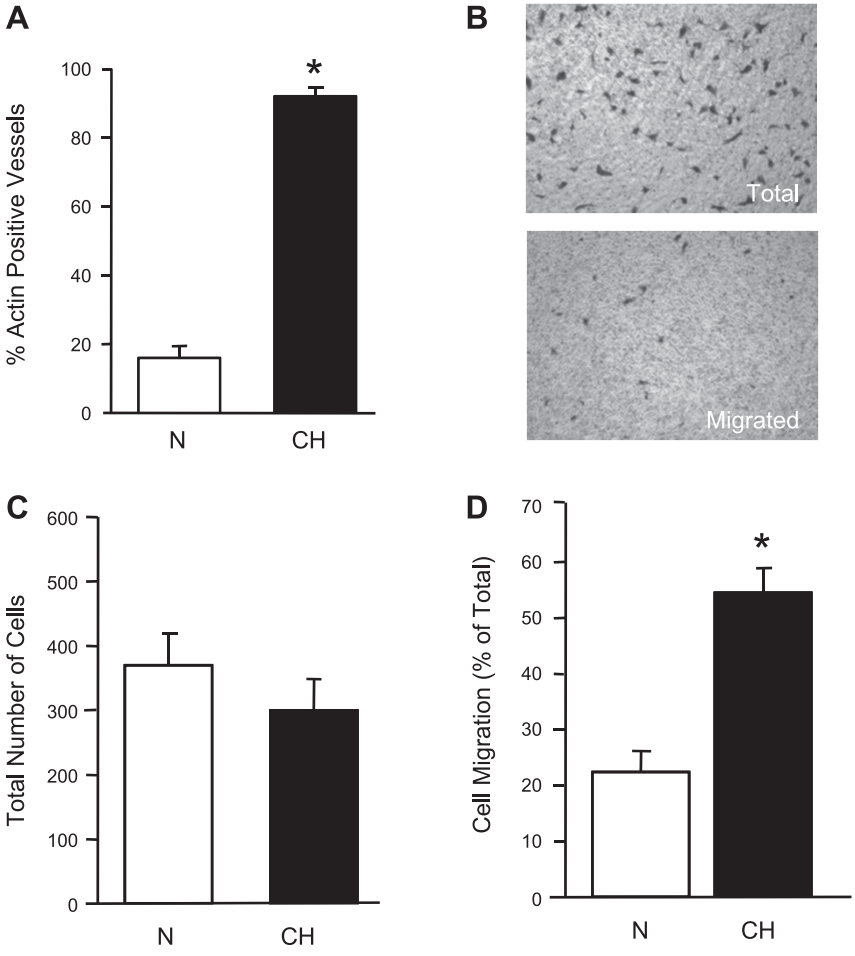

Fig. 1. Pulmonary vascular remodeling and pulmonary arterial smooth muscle cell (PASMC) migration in animals exposed to chronic hypoxia. *A*: bar graph showing mean ± SE for percent of small-diameter vessels (> 100 μm outer diameter) that stained positive for smooth muscle-specific α-actin (SMA) in normoxic (N) and chronically hypoxic (CH) rat lungs ($n = 5$ each). *B*: representative images showing total cells on the filter (*top*) and cells remaining (*bottom*, migrated) after scraping unmigrated cells from the top of the filter. *C*: bar graph showing total number of cells on the membrane (adherence) for PASMCs from N and CH animals ($n = 6$ each). *D*: bar graph representing cell migration (migrated cells as a percent of the total cells) in cells isolated from N and CH animals ($n = 6$ each). For all graphs, data are expressed as means ± SE. *Significant difference from normoxic value ($P < 0.05$).

diameter ≤100 μm) using confocal microscopy (Zeiss LSM-510). Vessels were randomly identified via light microscopy and then scanned at 560 nm to evaluate the presence of SMA. For each lung, 20 randomly selected vessels were scored and the percentage of SMA-positive vessels was calculated.

Drugs. Verapamil (VER) and SKF-96365 (SKF) were obtained from Sigma-Aldrich. Fura 2-AM was obtained from Molecular Probes. Stock solutions of SKF (10 mM in deionized H_2O) were prepared, divided into aliquots, and stored at −20°C until used. VER stock solution (10 mM in deionized H_2O) was prepared on the day of the experiment. All stock solutions were diluted to working concentrations in perfusate or medium on the day of experiment.

Statistical analysis. All values are expressed as means ± SE. For all experiments, cells isolated from different animals were used; thus *n* refers to both the number of independent experiments as well as the number of animals. For $[Ca^{2+}]_i$ measurements, data were collected from up to 30 cells, and the values averaged to obtain a single value for each experiment. Data were compared by unpaired Student's *t*-test (for two samples) or groupwise by using one-way ANOVA with a Holms-Sidak post hoc test to determine differences between groups. A *P* value <0.05 was accepted as statistically significant.

RESULTS

Effect of in vivo hypoxic exposure on PASMC migration. In vivo, evidence for PASMC migration in response to CH exposure can be observed by increased muscularization of small-diameter (<100 μm) vessels. In lungs from normoxic animals, only 20% of small-diameter vessels were positive for SMA, indicating a layer of smooth muscle (Fig. 1*A*). Consistent with previous results (2), exposure to CH (10% O_2; 3 wk) significantly increased the percent of SMA-positive vessels. To more directly assess the effect of chronic exposure to in vivo hypoxia on PASMC migration, cells were isolated from normoxic and chronically hypoxic rats and migration was measured via Transwell filter assay (Fig. 1*B*). The total number of cells on the filters was not significantly different for normoxia and CH (Fig. 1*C*), indicating similar levels of adherence between groups; however, PASMCs from chronically hypoxic rats exhibited significantly greater migration than PASMCs from normoxic rats (Fig. 1*D*).

AQP expression in PASMCs. To determine which AQP isoforms were present in PASMCs, we performed a screen of AQP mRNA expression in isolated PASMCs. AQP0 is restricted primarily to the eye, and AQP10–12 have not been found to be expressed in lung tissue (9). Screening for AQP1–9 via conventional PCR revealed that PASMCs exhibited robust expression of AQP1 mRNA, with lesser expression of mRNA for AQP4 and AQP7 (Fig. 2*A*). PASMCs did not express AQP2, 3, 5, 6, 8, or 9, although bands for these AQPs were clearly observed in control tissues, indicating that primer pairs and protocols were appropriate for detecting these mRNAs. A qualitatively similar pattern of AQP expression was observed in AoSMCs. The mRNA results for AQP1, AQP4, and AQP7 in PASMCs and AoSMCs were confirmed by immunoblot (Fig. 2*B*). Side-by-side analysis of protein expression revealed that the level of AQP1 and AQP7 protein expressed in both cell types was similar, whereas AoSMCs exhibited significantly higher levels of AQP4 protein than did PASMCs.

Effect of in vivo exposure to hypoxia on AQP expression in pulmonary vascular smooth muscle. After determining which AQPs were present in PASMCs, we performed experiments to determine the effect of in vivo exposure to hypoxia on AQP1

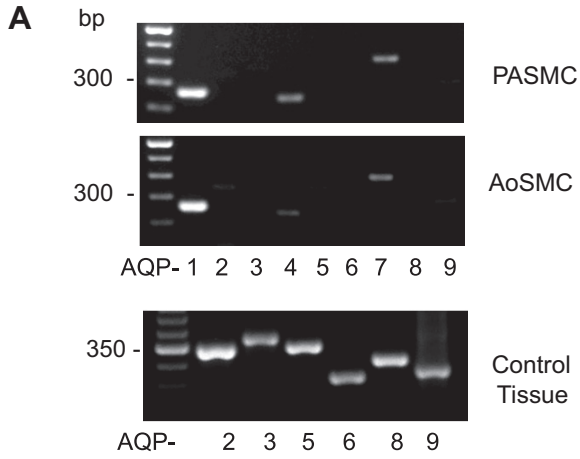

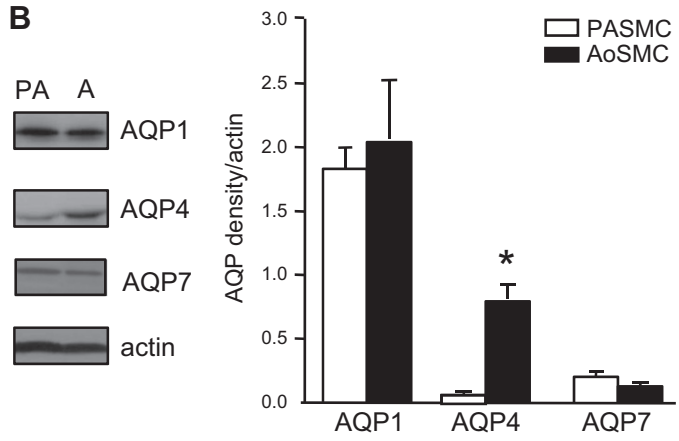

Fig. 2. Aquaporin (AQP) expression in pulmonary arterial and aortic smooth muscle cells. *A*: representative images from conventional PCR experiments showing products expressed in PASMCs (*top*) and aortic smooth muscle cells (AoSMCs; *middle*). Bottom image shows correct products were observed by using identical primers and conditions in control tissues (lung, kidney, or liver). *B*: representative immunoblots showing AQP1 (~26 kDa), AQP4 (~37 kDa), AQP7 (~30 kDa), and actin (~44 kDa) expression in PASMCs (PA) and AoSMCs (A). Results are representative of 3–5 experiments each. Bar graph shows mean ± SE protein levels (AQP/actin) in PASMCs and AoSMCs. *Significant difference from PASMCs.

lung levels. Lung AQP1 protein levels were increased by exposure to CH (Fig. 3, *A* and *B*), whereas AQP4 and AQP7 protein levels were unchanged. In contrast, the expression of AQP5, which is found primarily in epithelial cells, was markedly decreased by exposure to CH. To further isolate the effect of hypoxia to the smooth muscle, AQP protein levels were measured in endothelium-denuded intrapulmonary arteries from normoxic and chronically hypoxic rats. Similar to the results obtained in whole lung tissue, AQP1, but not AQP4 or AQP7, was significantly increased by CH in pulmonary arteries (Fig. 3*C*). Real-time PCR revealed that the increase in AQP1 protein levels after exposure to CH was correlated with a significant increase in AQP1 mRNA levels in these arteries (Fig. 3*D*), whereas mRNA levels for AQP4 and AQP7 were unchanged.

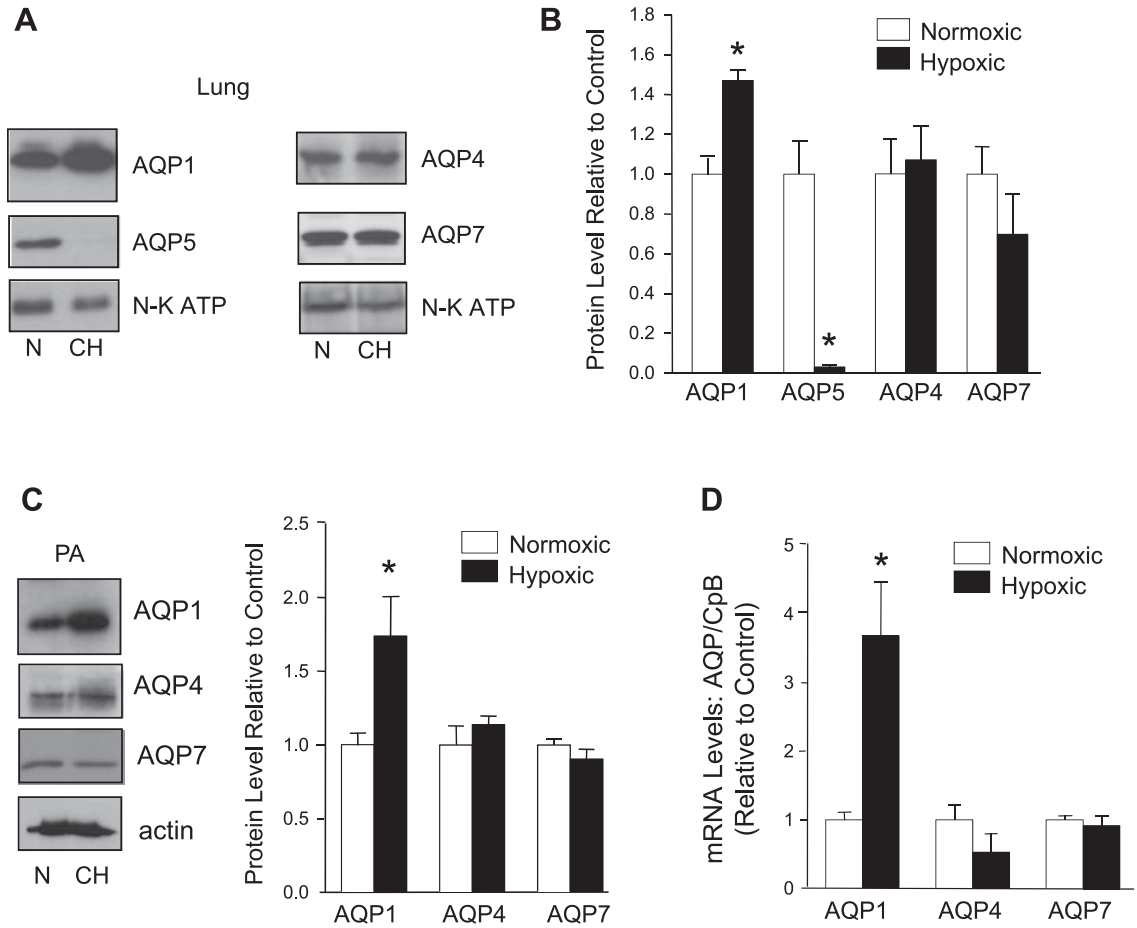

Fig. 3. Effect of hypoxia on AQP expression. *A*: immunoblots showing selective increase in AQP1 (~26 kDa) expression in lung homogenates from normoxic and chronically hypoxic rats. AQP levels were normalized by use of Na^+-K^+-ATPase (N-K ATP; ~110 kDa) as a loading control. *B*: bar graph shows AQP protein levels (normalized to N-K ATP); $n = 3$–6 rats/group. *C*: immunoblots demonstrating AQP1 (~26 kDa), AQP4 (~37 kDa), and AQP7 (~30 kDa) expression in endothelium-denuded PA from normoxic and chronically hypoxic rats. Bar graph shows AQP protein levels (normalized to actin); $n = 5$–6 each. *D*: bar graph showing real-time PCR results for AQP1, AQP4, and AQP7 mRNA levels (normalized to cyclophilin B; CpB) in PAs from N and CH rats. For all graphs, data are expressed as means ± SE. *Significantly different from normoxic ($P < 0.05$).

Ex vivo hypoxia and PASMC migration. The ability of hypoxia to induce PASMC migration independent of changes in hemodynamics or circulating factors was measured in PASMCs isolated from normoxic rats and exposed to hypoxia (4% O_2) ex vivo. In our experiments, these conditions did not cause proliferation (unpublished observations). Qualitative assessment of migration was performed via scratch wound assays. Images captured immediately after creating the wound and after 24 h of exposure to control conditions showed only a little movement of cells into the wound (Fig. 4*A*). In contrast, when cells were exposed to hypoxia, cells were clearly visible within the wound. Quantitative measures of migration were performed via Transwell assays (Fig. 4*B*). Exposure to hypoxia had no effect on adherence of cells to the membrane (Fig. 4*C*) but significantly increased PASMC migration (Fig. 4*D*). In AoSMCs, both adherence and percent migrating cells were similar under normoxic and hypoxic conditions.

Effect of ex vivo hypoxia on AQP1 expression. Since in vivo exposure to hypoxia was correlated with significant increases in AQP1 protein levels in pulmonary arteries, we determined the effect of ex vivo hypoxia on AQP1 expression in PASMCs. Surprisingly, ex vivo hypoxia had little effect on AQP1 protein levels in confluent cells (Fig. 5*A*). To test whether cell-to-cell contact could alter the response to hypoxia, we created "scratches" in the monolayers to approximate 50% confluence and create conditions that would allow the cells to migrate. Under these conditions, AQP1 protein levels increased under control conditions (although the difference did not reach statistical significance, $P = 0.063$), with a further increase observed with exposure to hypoxia. No effect of "scratching" or hypoxia was observed on AQP1 expression in AoSMCs (Fig. 5*B*). In contrast to the results observed with in vivo CH, short-term in vitro hypoxic exposure had no effect on AQP1 mRNA levels in PASMCs, regardless of whether the monolayers were intact or scratched (Fig. 5*C*).

Role of AQP1 in PASMC migration. To determine whether AQP1 was necessary for migration in PASMCs, siRNA was used to reduce AQP1 levels in PASMCs (Fig. 6, *A* and *B*). Compared with cells transfected with nontargeting siRNA, we were able to achieve an average of 70% reduction in AQP1 protein, with little effect on AQP4 protein levels (Fig. 6*B*), indicating selectivity of the siRNA. There was no significant difference in adherence in cells treated with nontargeting siRNA and siRNA directed against AQP1 (total cells: 396 ±

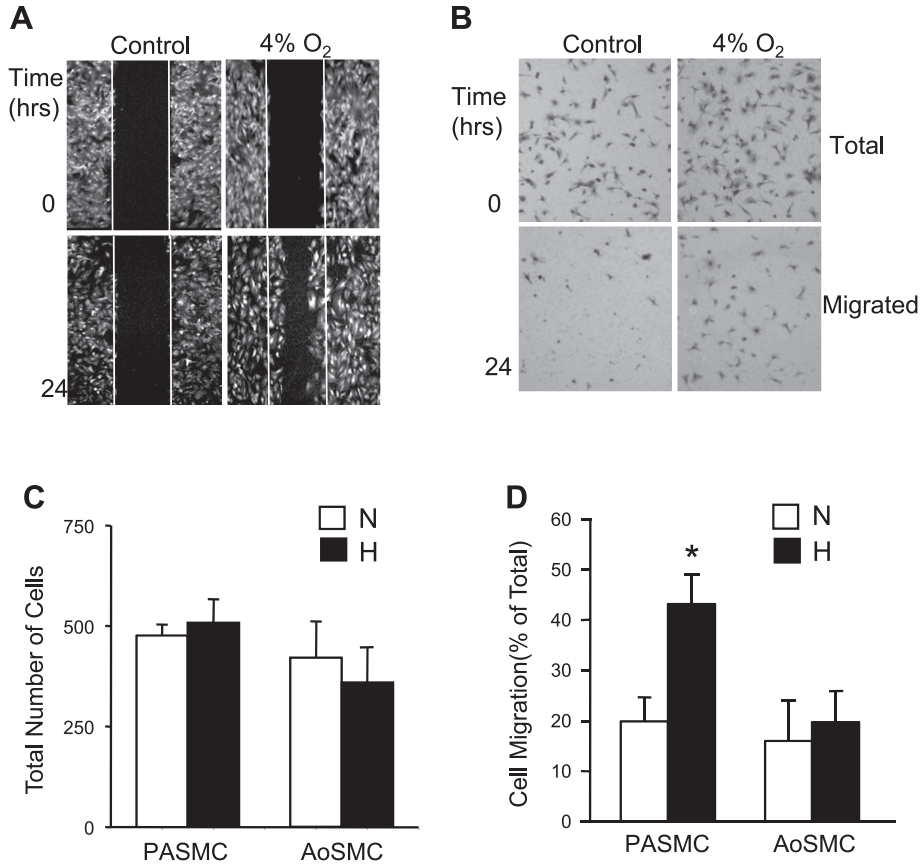

Fig. 4. Cell migration and proliferation in rat PASMCs exposed to normoxic (Control) and hypoxic (4% O_2) conditions for 24 h. *A*: PASMC migration visualized via "wound" or scratch motility assay. Images are representative of 3 separate experiments. *B*: PASMC migration assessed by Transwell assay. Panels show total number of cells on the membrane before and after scraping the top chamber (unmigrated cells). *C*: bar graphs shows total number of cells on the filter for PASMCS and AoSMCs exposed to normoxic and hypoxic (H; 4% O_2 for 24 h) conditions; $n = 6$ for PASMCs and $n = 4$ for AoSMCs. *D*: bar graph shows mean ± SE migration (normalized to total number of cells) in response to N or H; $n = 6$ for PASMCs, $n = 4$ for AoSMCs. *Significantly different from normoxic ($P < 0.05$).

38 vs. 423 ± 33, respectively; $n = 6$ each). Knockdown of AQP1 had no significant effect on PASMC migration under control conditions but completely prevented hypoxia-induced migration (Fig. 6*C*).

Role of calcium in hypoxia-induced migration. Intracellular calcium levels were measured in PASMCs exposed to hypoxia (4% O_2) for 15 min or 24 h and in PASMCs isolated from normoxic or chronically hypoxic rats (Fig. 7*A*). Baseline $[Ca^{2+}]_i$ levels in normoxic cells were similar across groups; however, in each case, hypoxia caused a significant increase in $[Ca^{2+}]_i$. A lack of increase in $[Ca^{2+}]_i$ in response to acute (15 min) hypoxic exposure has been previously demonstrated in AoSMCs (31). We tested whether a similar lack of response also occurred with more prolonged (24 h) exposure. We found that basal $[Ca^{2+}]_i$ levels were slightly lower in normoxic AoSMCs compared with PASMCs ($P < 0.05$), and no increase in $[Ca^{2+}]_i$ was observed in response to hypoxia (Fig. 7*B*).

Since these results suggested that $[Ca^{2+}]_i$ could be an initiating factor in migration, experiments were performed in the presence of calcium channel blockers to assess the contribution of Ca^{2+} influx to migration. Similar to our previous results with acute and prolonged hypoxia in vitro (32, 33), treatment with SKF (30 μM), a nonselective cation channel (NSCC) inhibitor, or VER (10 μM), a voltage-dependent calcium channel (VDCC) inhibitor, had no effect on basal $[Ca^{2+}]_i$ levels in nonhypoxic cells (Fig. 8*A*). In cells exposed to hypoxia (4% O_2; 24 h), both SKF and VER attenuated the increase in $[Ca^{2+}]_i$. Treatment with VER and SKF also prevented the hypoxia-induced increase in PASMC migration (Fig. 8*B*). Although VER appeared to decrease basal migration in normoxic PASMCs, the difference did not reach statistical significance. There was no significant difference in adherence between normoxic and hypoxic cells treated with either VER or SKF, so these values were grouped together for comparison across antagonist treatment. The total number of cells on the filter did not differ between Ca^{2+} channel antagonists (407 ± 56 for VER and 551 ± 78 for SKF; $n = 6$ each) and were not different compared with adherence in control cells (476 ± 28; $n = 6$). We next tested the effect of preventing Ca^{2+} influx on AQP1 expression. In "scratched" monolayers, hypoxia increased AQP1 protein levels in untreated cells (Fig. 8*C*). The hypoxia-induced increase in AQP1 protein levels was completely prevented in PASMCs treated with either VER or SKF.

DISCUSSION

In this study, we demonstrated that PASMCs express AQP1, AQP4, and AQP7 and exhibit an increase in $[Ca^{2+}]_i$, selective upregulation of AQP1 protein expression, and enhanced migration in response to hypoxia. The upregulation of AQP1 protein in response to hypoxia was dependent on Ca^{2+} influx through VDCCs and NSCCs and was required for hypoxia-induced PASMC migration. Although AoSMCs also express AQP1, AQP4, and AQP7, the hypoxia-induced increases in $[Ca^{2+}]_i$, AQP1 protein levels and migration are absent in this cell type. These results identify the AQPs present in pulmonary vascular smooth muscle and demonstrate an important role for AQP1 in mediating PASMC-specific effects of hypoxia.

It has long been recognized that structural remodeling is a key characteristic in the pulmonary vascular response to CH.

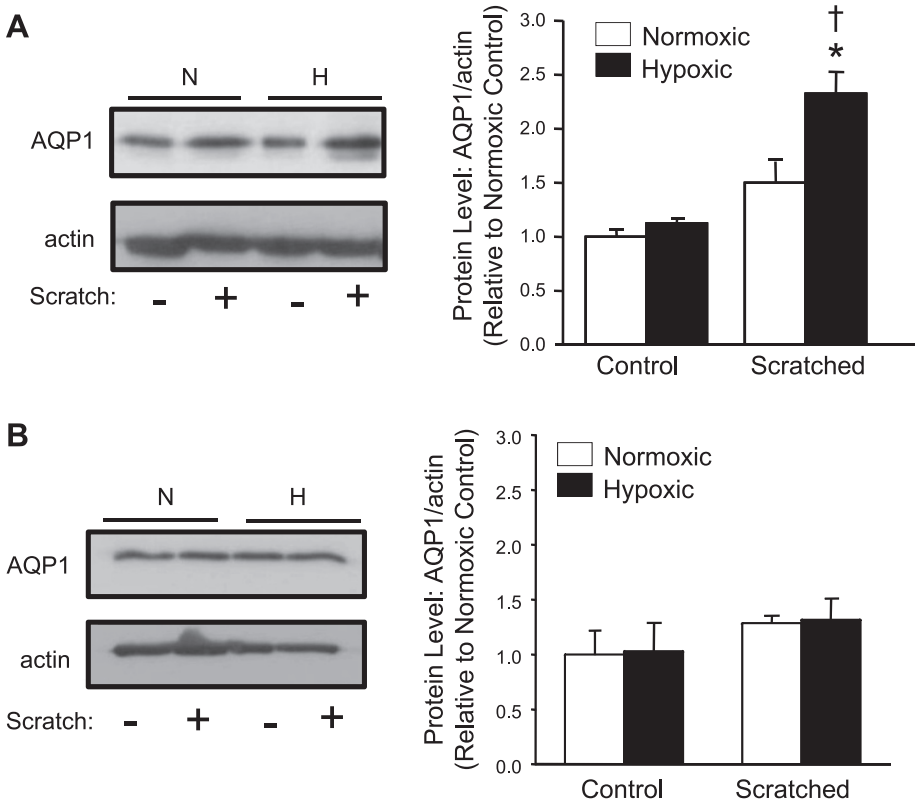

Fig. 5. Effect of hypoxia on AQP1 expression in vitro. Immunoblot assay shows AQP1 (~26 kDa) protein levels after exposure to normoxia or hypoxia (4% O_2 for 24 h) in undisturbed monolayers (control) of PASMCs (*A*) and AoSMCs (*B*), and when monolayers were scratched to remove ~50% of the cells. Bar graphs show data (normalized to normoxic control) from 3–4 separate experiments. *C*: real-time PCR results showing mRNA levels (AQP1/CpB) normalized to normoxic control (unscratched) in PASMCs ($n = 3$ each). For all graphs, data are expressed as means ± SE. *Significantly different from normoxic scratched ($P < 0.05$). †Significantly different from hypoxic control ($P < 0.05$).

Although proliferation and hypertrophy have been widely studied, the role of migration and factors governing this particular response has been less clear. In vivo, migration of PASMCs is likely to be a contributing factor to the extension of muscle down the vascular tree. After 3 wk of CH, there is a clear increase in muscularity of the small-diameter pulmonary vessels. Unfortunately, no specific markers of migrating cells have been identified, and the exact extent to which the development of new muscle is due to migration vs. proliferation remains to be determined. Nonetheless, using in vitro assays, we demonstrated that PASMCs derived from chronically hypoxic rats exhibit enhanced migratory capacity under basal conditions that persisted even after return to normoxic conditions for 2–3 days. These data support the possibility of a role of migration in the in vivo response. The ability of hypoxia to induce PASMC migration does not appear to require exposure to increased mechanical stress (i.e., elevated pulmonary arterial pressures) or elevated levels of circulating factors, since PASMCs isolated from normoxic animals and subjected to ex vivo hypoxia also responded with an increase in migration. These data indicate that the mechanism for inducing migration in response to hypoxia exists within the PASMCs, although it is possible that external influences may modify or accentuate the response in vivo.

Accumulating evidence indicates that migration of certain cell types is regulated by AQP1 (13). The identity of AQPs expressed in vascular smooth muscle is not well characterized. Although AQP1 has been described in AoSMCs and coronary smooth muscle cells (20), reports of other AQP isoforms in vascular smooth muscle are lacking. We found that PASMCs expressed both mRNA and protein for AQP1, AQP4, and AQP7; a similar distribution was observed in AoSMC. Interestingly, direct comparison between PASMCs and AoSMCs revealed that whereas AQP1 and AQP7 levels were similar

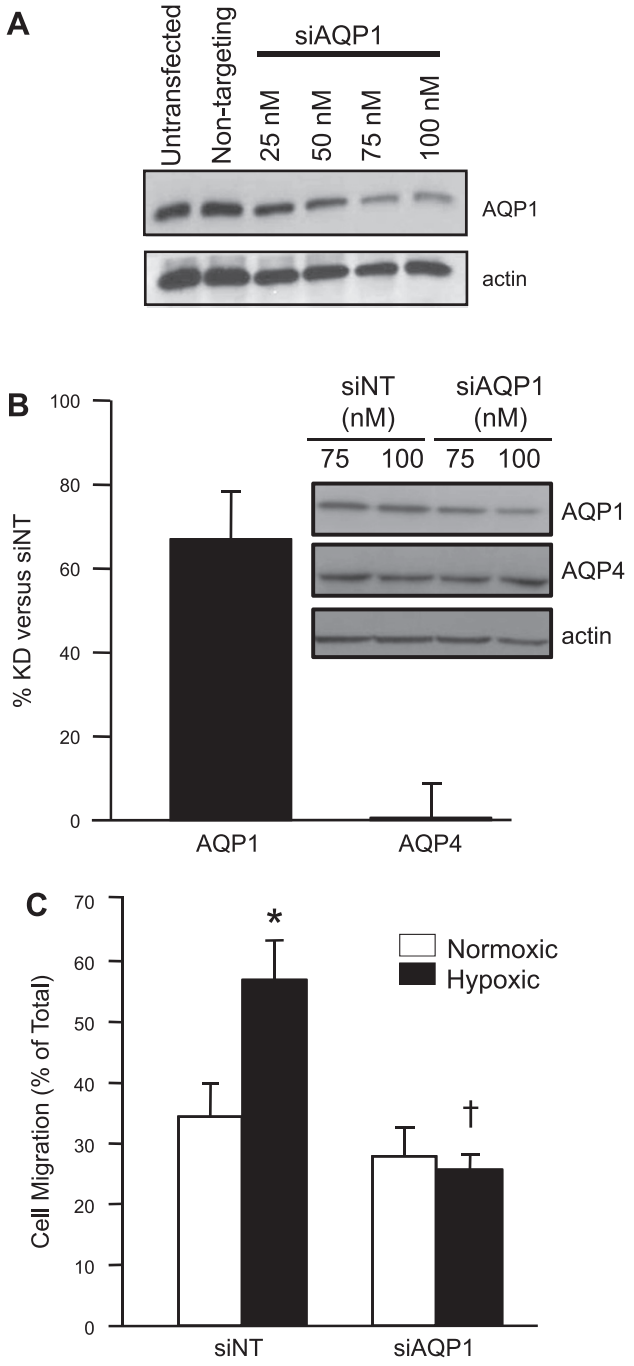

Fig. 6. Effect of AQP1 depletion on PASMC migration. *A*: immunoblot images showing initial experiments to determine optimal small interfering RNA (siRNA) concentrations for cells transfected with silencing RNAs targeting AQP1 (siAQP1) or nontargeting siRNA (siNT). *B*: treatment with siAQP1 (100 nM) reduced AQP1 (~26 kDa) expression in PASMCs, but had no significant effect on AQP4 (~37 kDa) expression. Bar graph shows the average amount of knockdown vs. siNT for AQP1 and AQP4 protein normalized to actin ($n = 4$). *C*: bar graph showing percent migration for PASMCs transfected with siNT and siAQP1 and exposed to normoxic or hypoxic (4% O_2; 24 h) conditions ($n = 6$ each). For all graphs, data are expressed as means ± SE. *Significantly different from siNT normoxic ($P < 0.05$). †Significantly different from siNT hypoxic ($P < 0.05$).

between these cell types, PASMCs exhibited much less AQP4 protein than did AoSMCs. Whether this represents a consistent finding across smooth muscle from other vascular beds and results in a functional difference between these cell types remains to be determined.

The regulation of AQP expression by hypoxia appears to be controlled on several levels and in an isoform-selective manner. Exposure to hypoxia, either in vivo or in vitro, resulted in a marked upregulation of AQP1 protein. The effect of hypoxia was selective for the AQP1 isoform, since neither AQP4 nor AQP7 exhibited increased mRNA or protein expression with in vivo hypoxic exposure, and AQP5 protein, which is found primarily in epithelial cells (11, 14), was dramatically reduced in chronically hypoxic lungs. Whether the downregulation of AQP5 by hypoxia was due to a differential response of AQP5 or epithelial cells to low-oxygen conditions remains to be determined. With short-term ex vivo hypoxic exposure, the increase in AQP1 protein levels was not accompanied by a change in mRNA levels, suggesting that the induction of protein under these conditions occurred via posttranslational mechanisms, whereas with prolonged in vivo hypoxia AQP1 mRNA levels were increased significantly, indicating that AQP1 levels under these conditions may also be under transcriptional control. The AQP1 promoter has been shown to have a putative binding site for the oxygen-sensitive transcription factor hypoxia-inducible factor (HIF), and data now indicate that AQP1 can be regulated by HIF in a glioma cell line (1) and in retinal vascular endothelial cells (26). Further experiments will be required to determine whether the upregulation of AQP1 mRNA levels observed in pulmonary arterial smooth muscle from chronically hypoxic rats is HIF dependent. With respect to the other AQP isoforms, little is known about the hypoxic regulation of AQP5 and AQP7, although hypoxia has been shown to decrease AQP4 mRNA levels in astrocytes (34). Although there was a trend toward reduced AQP4 mRNA in pulmonary arteries from chronically hypoxic rats, this did not reach statistical significance and was not reflected as a reduction in AQP4 protein levels. In contrast to the results obtained in PASMCs, we found that hypoxia had no effect on AQP1 protein levels in AoSMCs. Taken together, these data indicate that AQP isoforms exhibit differential regulation by hypoxia and that the effects of hypoxia on AQP1 and AQP4 are cell type specific.

The increase in AQP1 protein levels that occurred in PASMCs during in vitro exposure to hypoxia was dependent on the increase in $[Ca^{2+}]_i$ that occurs in these cells. Blockade of Ca^{2+} influx through either VDCCs or NSCCs completely prevented the rise in resting $[Ca^{2+}]_i$ induced by hypoxia, as well as the increase in AQP1 protein levels. Although SKF can block VDCCs in some instances, we have previously demonstrated that the concentration used in this study had no effect on depolarization-induced calcium influx in our cell type (38). In AoSMCs, hypoxia caused neither an increase in $[Ca^{2+}]_i$, nor increased AQP1 protein expression, further confirming that the $[Ca^{2+}]_i$ response to hypoxia, and subsequent elevation in AQP1 expression, varies across cell types. Our results are consistent with a report in prostate cancer cells, where elevated AQP1 expression was decreased in the presence of verapamil (27).

The mechanism by which the hypoxia-induced increase in $[Ca^{2+}]_i$ regulates AQP1 levels is not known. Since mRNA

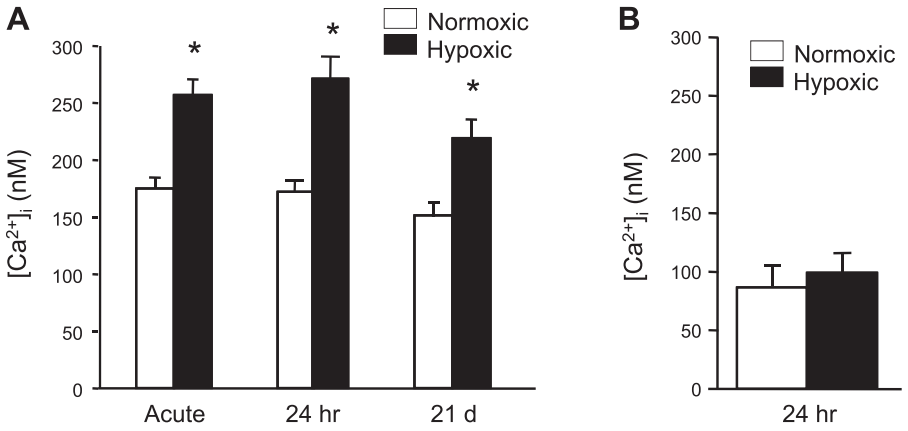

Fig. 7. Basal intracellular calcium concentration ($[Ca^{2+}]_i$) in PASMCs exposed to hypoxia. *A*: resting $[Ca^{2+}]_i$ in PASMCs exposed to normoxia or hypoxia (4% O_2) for 15 min (acute) or 24 h or isolated from animals exposed to hypoxia (inspired O_2 fraction = 10%) for 21 days (d); $n = 3–6$ each. *B*: resting, basal $[Ca^{2+}]_i$ in AoSMCs exposed to normoxia or hypoxia (4% O_2) for 24 h; $n = 3$ each. Data are expressed as means ± SE. *Significantly different from normoxic at same time point ($P < 0.05$).

levels were not altered during acute hypoxic exposure, it is unlikely that changes in AQP1 transcription are involved; these changes may instead be a result of altered AQP1 protein synthesis and/or stability. In fibroblasts, posttranslational regulation of AQP1 abundance has been described in response to hypertonic stress, which decreased ubiquitination and proteasomal degradation of the protein (12). Moreover, hypertonic stress has been shown to increase $[Ca^{2+}]_i$ in fibroblasts (17) and other investigators have reported that ubiquitin ligase activity can be altered by changes in $[Ca^{2+}]_i$ (3, 30). Whether hypoxia or increased $[Ca^{2+}]_i$ regulate AQP1 ubiquitination in PASMCs remains to be determined. In addition to ubiquitination, protein abundance could also be modulated by localization within the cell. Recently, hypotonic stress was found to induce AQP1 translocation via a Ca^{2+}-dependent mechanism in astrocytes (4), resulting in insertion of the protein into the

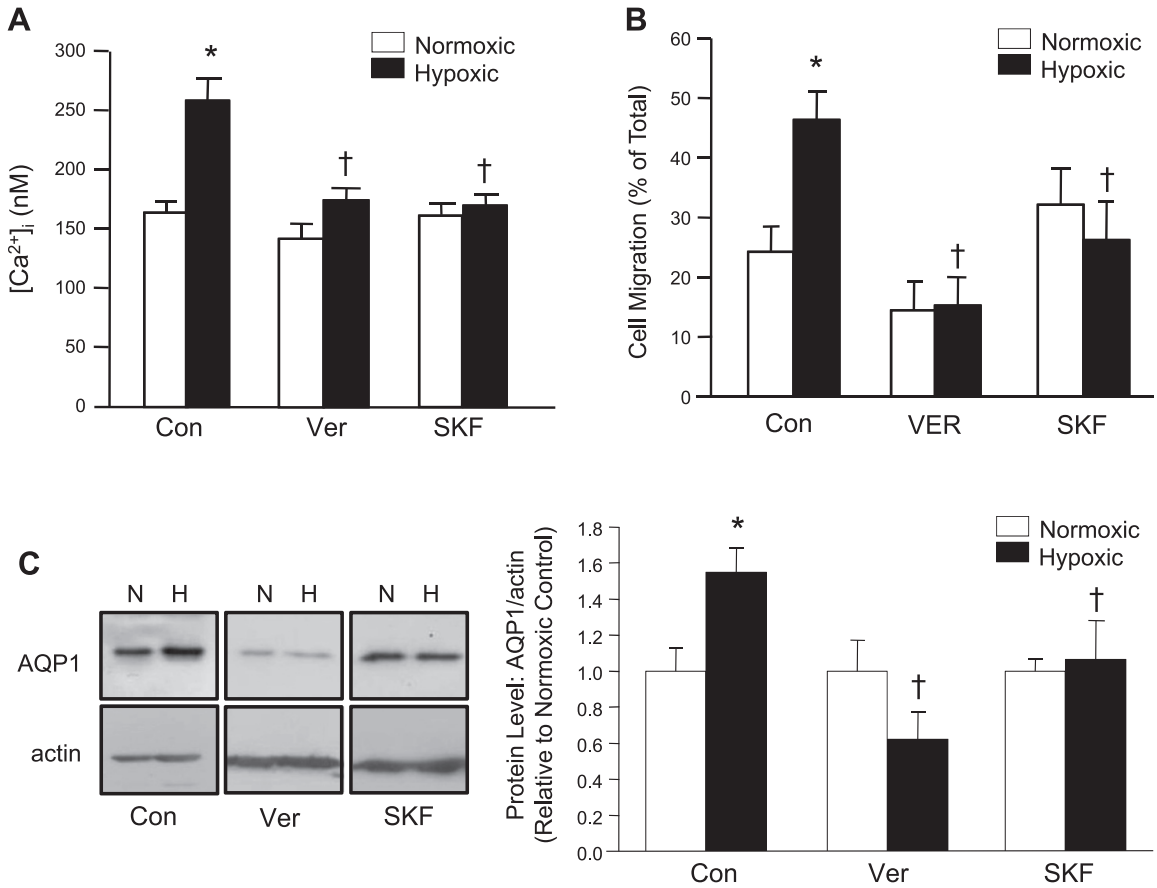

Fig. 8. Role of $[Ca^{2+}]_i$ in cell migration and AQP1 expression. *A*: bar graph shows resting $[Ca^{2+}]_i$ in PASMCs exposed to normoxia or hypoxia (4% O_2 for 24 h) under control conditions (Con) or in the presence of verapamil (VER; 10 mM), a voltage-dependent calcium channel inhibitor, or SKF-96365 (SKF; 30 μM), a nonselective cation channel inhibitor ($n = 3–6$ each). *B*: bar graph shows the percent migration for PASMCs exposed to normoxia or hypoxia under control conditions or in the presence of SKF or VER ($n = 4–6$ each). *C*: representative immunoblot images and bar graph ($n = 3$ each) show AQP1 (~26 kDa) protein levels in scratched monolayers exposed to normoxia or hypoxia under control conditions or in the presence of SKF or VER. For all graphs, data are expressed as means ± SE. *Significantly different from normoxic Con ($P < 0.05$). †Significantly different from hypoxic Con ($P < 0.05$).

membrane. Whether Ca^{2+}-dependent translocation and membrane insertion of AQP1 also results in increased protein stability is unknown, although studies of AQP5 in lung epithelial cells suggest that protein abundance was directly related to Ca^{2+}-dependent internalization followed by lysosomal degradation (22), providing corroborative evidence that membrane insertion could increase protein abundance. Since the COOH-terminal tail of AQP1 contains a putative E-F hand motif (6), the possibility also exists that Ca^{2+} could bind directly to AQP1 and regulate protein localization and/or stability, although future experiments will be required to test this hypothesis.

Our experiments with confluent monolayers vs. monolayers where ~50% of the cells had been removed revealed that cell-to-cell contact in confluent monolayers exerts an inhibitory effect on AQP1 protein expression. Removing cells had no effect on AQP1 mRNA expression, indicating that contact-dependent repression of AQP1 was not occurring at the transcriptional level. Cell density has been shown to alter AQP1 protein levels in other cell types, since sparsely plated tumor cells exhibited less AQP1 protein than densely plated cells (27). Although these results are opposite of those found in PASMCs, the difference in results could be due to cell-specific responses or differences in the methods used to measure protein expression (immunoblot vs. immunofluorescence).

That silencing of AQP1 or preventing the hypoxia-induced increase in AQP1 protein by Ca^{2+} channel inhibitors completely blocked the enhanced migration of PASMCs observed under hypoxic conditions underscores the importance of AQP1 in mediating this response. The exact mechanisms by which AQP1 facilitates hypoxia-induced migration are unclear. In endothelial cells, AQP1 was shown to colocalize to the lamellipodia (18), which was proposed to allow localized movement of water across the cell membrane, resulting in directed cell movement. Another possibility is that AQP1 is required for cytoskeletal rearrangement. Recent evidence in human melanoma and endothelial cell lines indicates that loss of AQP1 was associated with decreased levels of Lin7 and β-catenin, proteins that serve as scaffolding complexes and aid in cytoskeletal anchoring (13). Determining whether the mechanism by which AQP1 mediates hypoxia-induced migration in PASMCs involves localized control of water flux and/or regulation of the actin cytoskeleton is an area of continuing investigation.

In summary, we found that AQP1, AQP4, and AQP7 are expressed in both PASMCs and AoSMCs; however, only AQP1 is upregulated by hypoxia, and only in PASMCs. Hypoxia-induce migration occurred in PASMCs, but not the AoSMCs, and was prevented by depletion of AQP1 or by preventing the hypoxia-induced increase in AQP1 with calcium channel blockers. Similar increases in AQP1 expression in PASMCs were observed with in vivo exposure to CH, suggesting a possible role of AQP1 in mediating pulmonary vascular remodeling during the pathogenesis of pulmonary hypertension. Our findings provide new insight into the function of AQP1 in PASMCs and further our understanding of the mechanisms by which CH may lead to PASMC migration.

GRANTS

This work was supported by grants from the American Heart Association Mid-Atlantic Affiliate (Grant-in-Aid AHA0755479) and the National Institutes of Health (HL-07963).

DISCLOSURES

No conflicts of interest, financial or otherwise, are declared by the author (s).

REFERENCES

1. **Abreu-Rodriguez I, Sanchez Silva R, Martins AP, Soveral G, Toledo-Aral JJ, Lopez-Barneo J, Echevarria M.** Functional and transcriptional induction of aquaporin-1 gene by hypoxia; analysis of promoter and role of HIF-1α. *PLoS One* 6: e28385, 2011.
2. **Abud EM, Maylor J, Undem C, Punjabi A, Zaiman AL, Myers AC, Sylvester JT, Semenza GL, Shimoda LA.** Digoxin inhibits development of hypoxic pulmonary hypertension in mice. *Proc Natl Acad Sci USA* 109: 1239–1244, 2012.
3. **Chen BB, Coon TA, Glasser JR, Mallampalli RK.** Calmodulin antagonizes a calcium-activated SCF ubiquitin E3 ligase subunit, FBXL2, to regulate surfactant homeostasis. *Mol Cell Biol* 31: 1905–1920, 2011.
4. **Conner MT, Conner AC, Bland CE, Taylor LH, Brown JE, Parri HR, Bill RM.** Rapid aquaporin translocation regulates cellular water flow: the mechanism of hypotonicity-induced sub-cellular localization of the aquaporin 1 water channel. *J Biol Chem* 287: 11516–11525, 2012.
5. **Cornfield DN, Stevens T, McMurtry IF, Abman SH, Rodman DM.** Acute hypoxia increases cytosolic calcium in fetal pulmonary artery smooth muscle cells. *Am J Physiol Lung Cell Mol Physiol* 265: L53–L56, 1993.
6. **Fotiadis D, Suda K, Tittmann P, Jeno P, Philippsen A, Muller DJ, Gross H, Engel A.** Identification and structure of a putative Ca^{2+}-binding domain at the C terminus of AQP1. *J Mol Biol* 318: 1381–1394, 2002.
7. **Hayashi S, Takahashi N, Kurata N, Yamaguchi A, Matsui H, Kato S, Takeuchi K.** Involvement of aquaporin-1 in gastric epithelial cell migration during wound repair. *Biochem Biophys Res Commun* 386: 483–487, 2009.
8. **Hu J, Verkman AS.** Increased migration and metastatic potential of tumor cells expressing aquaporin water channels. *FASEB J* 20: 1892–1894, 2006.
9. **Ishibashi K, Hara S, Kondo S.** Aquaporin water channels in mammals. *Clin Exp Nephrol* 13: 107–117, 2009.
10. **King LS, Nielsen S, Agre P.** Aquaporin-1 water channel protein in lung: ontogeny, steroid-induced expression, and distribution in rat. *J Clin Invest* 97: 2183–2191, 1996.
11. **Kreda SM, Gynn MC, Fenstermacher DA, Boucher RC, Gabriel SE.** Expression and localization of epithelial aquaporins in the adult human lung. *Am J Respir Cell Mol Biol* 24: 224–234, 2001.
12. **Leitch V, Agre P, King LS.** Altered ubiquitination and stability of aquaporin-1 in hypertonic stress. *Proc Natl Acad Sci USA* 98: 2894–2898, 2001.
13. **Monzani E, Bazzotti R, Perego C, La Porta CA.** AQP1 is not only a water channel: it contributes to cell migration through Lin7/beta-catenin. *PLoS One* 4: e6167, 2009.
14. **Nielsen S, King LS, Christensen BM, Agre P.** Aquaporins in complex tissues. II. Subcellular distribution in respiratory and glandular tissues of rat. *Am J Physiol Cell Physiol* 273: C1549–C1561, 1997.
15. **Papadopoulos MC, Saadoun S, Verkman AS.** Aquaporins and cell migration. *Pflügers Arch* 456: 693–700, 2008.
16. **Pfaffl MW.** A new mathematical model for relative quantification in real-time RT-PCR. *Nucleic Acids Res* 29: e45, 2001.
17. **Potthast R, Abbey-Hosch SE, Antos LK, Marchant JS, Kuhn M, Potter LR.** Calcium-dependent dephosphorylation mediates the hyperosmotic and lysophosphatidic acid-dependent inhibition of natriuretic peptide receptor-B/guanylyl cyclase-B. *J Biol Chem* 279: 48513–48519, 2004.
18. **Saadoun S, Papadopoulos MC, Hara-Chikuma M, Verkman AS.** Impairment of angiogenesis and cell migration by targeted aquaporin-1 gene disruption. *Nature* 434: 786–792, 2005.
19. **Sham JS, Crenshaw BR Jr, Deng LH, Shimoda LA, Sylvester JT.** Effects of hypoxia in porcine pulmonary arterial myocytes: roles of K_V channel and endothelin-1. *Am J Physiol Lung Cell Mol Physiol* 279: L262–L272, 2000.
20. **Shanahan CM, Connolly DL, Tyson KL, Cary NR, Osbourn JK, Agre P, Weissberg PL.** Aquaporin-1 is expressed by vascular smooth muscle cells and mediates rapid water transport across vascular cell membranes. *J Vasc Res* 36: 353–362, 1999.
21. **Shimoda LA, Undem C.** Interactions between calcium and reactive oxygen species in pulmonary arterial smooth muscle responses to hypoxia. *Respir Physiol Neurobiol* 174: 221–229, 2010.

22. **Sidhaye VK, Schweitzer KS, Caterina MJ, Shimoda L, King LS.** Shear stress regulates aquaporin-5 and airway epithelial barrier function. *Proc Natl Acad Sci USA* 105: 3345–3350, 2008.
23. **Stenmark KR, McMurtry IF.** Vascular remodeling versus vasoconstriction in chronic hypoxic pulmonary hypertension: a time for reappraisal? *Circ Res* 97: 95–98, 2005.
24. **Stenmark KR, Meyrick B, Galie N, Mooi WJ, McMurtry IF.** Animal models of pulmonary arterial hypertension: the hope for etiological discovery and pharmacological cure. *Am J Physiol Lung Cell Mol Physiol* 297: L1013–L1032, 2009.
25. **Sylvester JT, Shimoda LA, Aaronson PI, Ward JP.** Hypoxic pulmonary vasoconstriction. *Physiol Rev* 92: 367–520, 2012.
26. **Tanaka A, Sakurai K, Kaneko K, Ogino J, Yagui K, Ishikawa K, Ishibashi T, Matsumoto T, Yokote K, Saito Y.** The role of the hypoxia-inducible factor 1 binding site in the induction of aquaporin-1 mRNA expression by hypoxia. *DNA Cell Biol* 30: 539–544, 2011.
27. **Tie L, Lu N, Pan X, Pan Y, An Y, Gao J, Lin Y, Yu H, Li X.** Hypoxia-induced up-regulation of aquaporin-1 protein in prostate cancer cells in a p38-dependent manner. *Cell Physiol Biochem* 29: 269–280, 2012.
28. **Vadula MS, Kleinman JG, Madden JA.** Effect of hypoxia and norepinephrine on cytoplasmic free Ca^{2+} in pulmonary and cerebral arterial myocytes. *Am J Physiol Lung Cell Mol Physiol* 265: L591–L597, 1993.
29. **Voelkel NF, Tuder RM.** Hypoxia-induced pulmonary vascular remodeling: a model for what human disease? *J Clin Invest* 106: 733–738, 2000.
30. **Wang J, Peng Q, Lin Q, Childress C, Carey D, Yang W.** Calcium activates Nedd4 E3 ubiquitin ligases by releasing the C2 domain-mediated auto-inhibition. *J Biol Chem* 285: 12279–12288, 2010.
31. **Wang J, Shimoda LA, Weigand L, Wang W, Sun D, Sylvester JT.** Acute hypoxia increases intracellular [Ca^{2+}] in pulmonary arterial smooth muscle by enhancing capacitative Ca^{2+} entry. *Am J Physiol Lung Cell Mol Physiol* 288: L1059–L1069, 2005.
32. **Wang J, Weigand L, Lu W, Sylvester JT, Semenza GL, Shimoda LA.** Hypoxia inducible factor 1 mediates hypoxia-induced TRPC expression and elevated intracellular Ca^{2+} in pulmonary arterial smooth muscle cells. *Circ Res* 98: 1528–1537, 2006.
33. **Whitman EM, Pisarcik S, Luke T, Fallon M, Wang J, Sylvester JT, Semenza GL, Shimoda LA.** Endothelin-1 mediates hypoxia-induced inhibition of voltage-gated K^+ channel expression in pulmonary arterial myocytes. *Am J Physiol Lung Cell Mol Physiol* 294: L309–L318, 2008.
34. **Yamamoto N, Yoneda K, Asai K, Sobue K, Tada T, Fujita Y, Katsuya H, Fujita M, Aihara N, Mase M, Yamada K, Miura Y, Kato T.** Alterations in the expression of the AQP family in cultured rat astrocytes during hypoxia and reoxygenation. *Brain Res Mol Brain Res* 90: 26–38, 2001.
35. **Zheng YM, Wang QS, Liu QH, Rathore R, Yadav V, Wang YX.** Heterogeneous gene expression and functional activity of ryanodine receptors in resistance and conduit pulmonary as well as mesenteric artery smooth muscle cells. *J Vasc Res* 45: 469–479, 2008.